

Supplementary Information for Universality in Coalescence of Polymeric Fluids

Sarath Chandra Varma,^a Aniruddha Saha,^b Siddhartha Mukherjee,^{b,c} Aditya Bandopadhyay,^b Alope Kumar,^a and Suman Chakraborty,^{* b,c}

^aDepartment of Mechanical Engineering, Indian Institute of Science, Bengaluru, Karnataka-560012, India. Tel: +91 80-22932958; E-mail: alokekumar@iisc.ac.in

^bDepartment of Mechanical Engineering, Indian Institute of Technology Kharagpur, West Bengal-721302, India

^cAdvanced Technology Development Center, Indian Institute of Technology Kharagpur, West Bengal-721302, India. Tel: +91 3222-282990; E-mail: suman@iitkgp.mech.ac.in

1 Critical and entanglement concentrations

Drastic alteration in the rheological behavior of the polymer solution can be observed depending on the polymer concentration c . Polymer solutions are classified as dilute, semi-dilute unentangled and semi-dilute entangled based on their critical concentration c^* . For PEO, PVA and PEG we calculate c^* from their intrinsic viscosities $[\eta]$ using the Flory relation $c^* = 1/[\eta]$. For PAM, c^* is calculated using $c^* = 3M_w/4\pi R_g^3 N_A$, where R_g is radius of gyration determined using $\langle R_g^2 \rangle^{1/2} = 0.0749M_w^{0.64} \text{Å}^1$ and N_A is Avogadro number. Intrinsic viscosity for the polymers are determined using the Mark-Houwink-Sakurada correlation $[\eta] = KM_w^b$ where, K is constant, M_w is molecular weight of the polymer and b is the exponent. The values of K and b for each polymer used are given in Table-S1. The critical concentration for PEG obtained from

Table S1 Mark-Houwink-Sakurada parameters for polymers

Polymer	K	b
PAM ¹	0.00933	0.75
PEO ²	0.072	0.65
PVA ³	0.00138	0.56
PEG ⁴	0.0224	0.73

the correlations is validated by plotting the specific viscosity η_{sp} with c as shown in Fig.S1a. It is observed that η_{sp} for concentrations less than 1 and greater than 1 have different slopes and both lines meet at a point with concentration of 5.2% w/v which gives us c^* and is in good agreement with the calculated value of 5.3% w/v obtained from correlation. The entanglement concentration for PEO is $c_e \approx 6c^{*5}$ which gives a value of 0.43% w/v. Concentrations of 0.5% and 0.6% were chosen for PEO for the experiments which fall in the semi-dilute entanglement regime. The theoretical entanglement concentration of 0.43% w/v has been experimentally validated by plotting η_{sp} with c as shown in Fig.S1b showing the deviation of specific viscosity values after 0.4% w/v concentration.

2 Rheological characterization of polymer solutions

The variation of viscosity for PAM, PEO, PVA and PEG are shown in Fig.S2. Shear thinning behavior is observed for PAM and PEO whereas, PVA and PEG showed the constant viscosity with shear rate $\dot{\gamma}$. Zero shear viscosity of the PAM solutions are obtained by fitting the rheology data in the form of Carreau-Yasuda model⁶ represented in equation $\eta - \eta_\infty = (\eta_o - \eta_\infty) [1 + (\Gamma \dot{\gamma})^a]^{n-1/a}$, where η_o , η_∞ , $\dot{\gamma}$, n , Γ and a represent zero-shear viscosity, infinite-shear viscosity, shear rate, flow behavior index, time constant and width of the transition region between η_o and the power-law region respectively. To characterize the viscoelastic behaviour of the polymer solutions SAOS experiments have been performed. The variation of storage modulus G' and loss modulus G'' with shear strain γ is shown in Fig.S3a for 0.3% w/v PEO and 24% w/v PEG. Similarly, the variation of G' and G'' with angular frequency ω (s^{-1}) for 0.4% w/v and 0.6% w/v PEO.

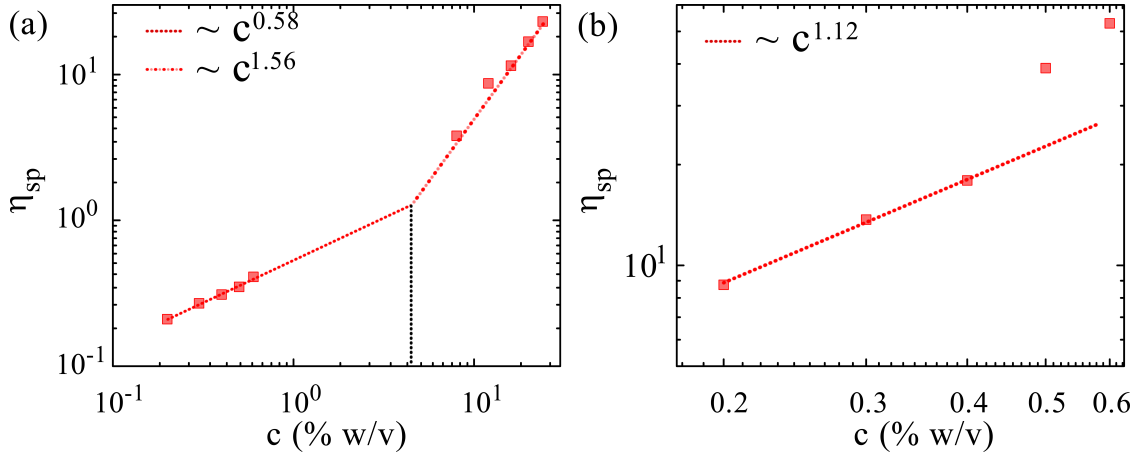


Fig. S1 Variation of specific viscosity with concentration for (a) PEG and (b) PEO.

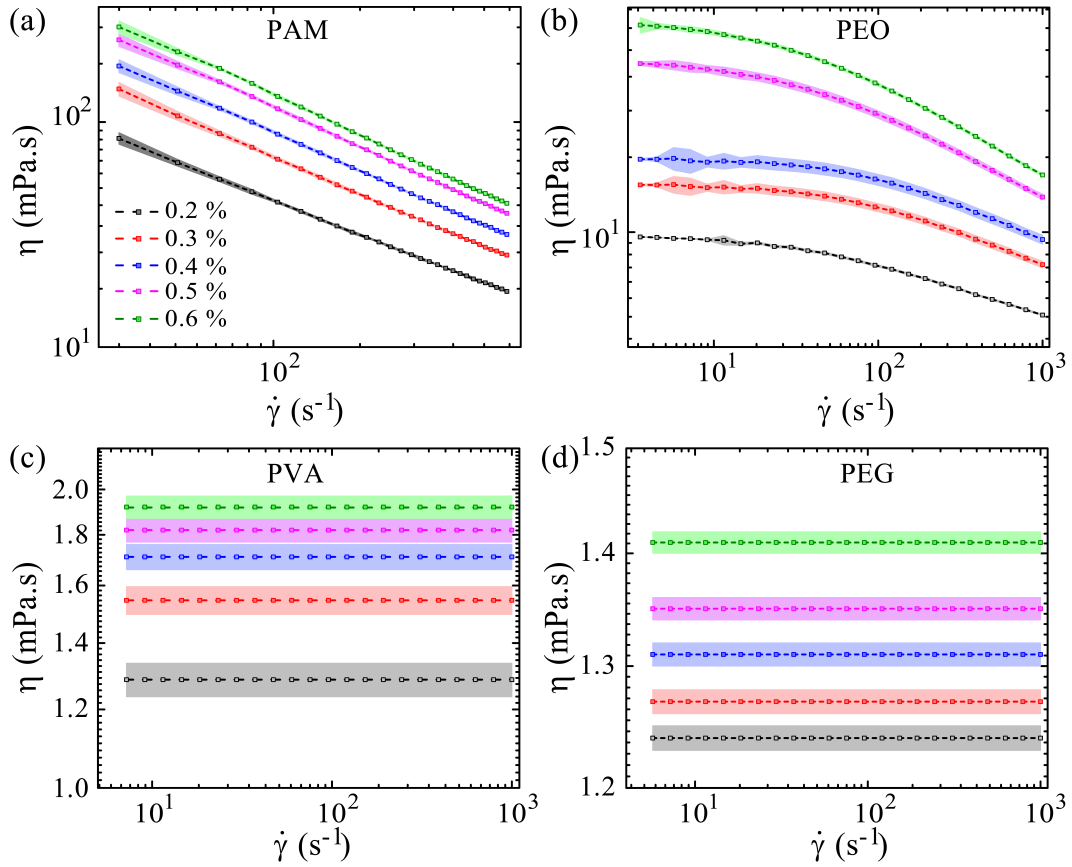


Fig. S2 Rheological behavior of (a) PAM, (b) PEO, (c) PVA and (d) PEG with representation of standard deviations using shades for the concentrations provided in the legend.

3 Relaxation times

Relaxation time of the dilute polymer solutions is obtained by using Zimm model⁶.

$$\lambda_z = \frac{1}{\zeta(3\nu)} \frac{[\eta]M_w\eta_s}{N_A k_B T} \quad (1)$$

where, λ_z is the Zimm relaxation time, η_s is the solvent viscosity, k_B is the Boltzmann constant, T is the absolute temperature and ν is fractal polymer dimension determined using the relation $b = 3\nu - 1$, where b is the exponent of Mark-Houwink-Sakurada correlation. However, the relaxation times of the solutions in semi-dilute unentangled λ_{SUE}

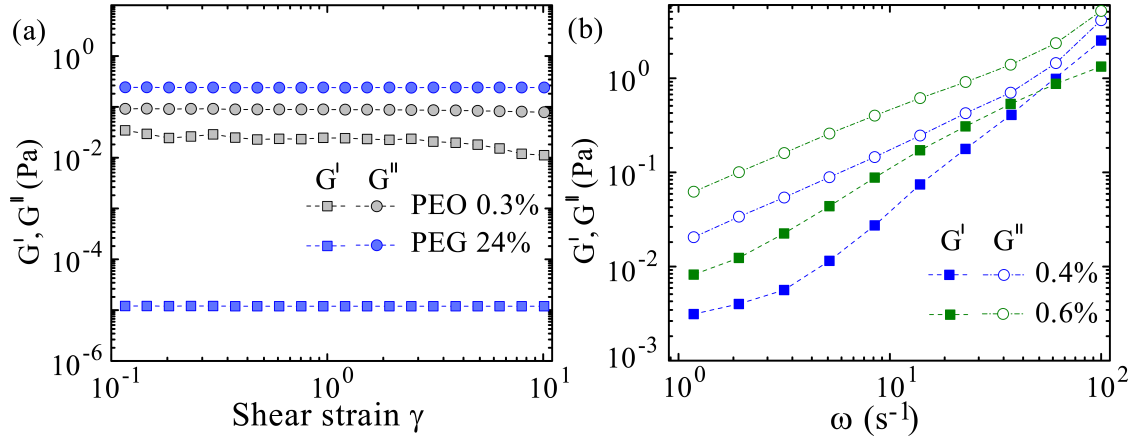


Fig. S3 Behavior of storage and loss modulus with (a) Shear strain for 0.3% w/v PEO and % w/v PEG and (b) angular frequency for 0.4% w/v and 0.6% w/v PEO.

and semi-dilute entangled λ_{SE} regimes solutions are calculated using these correlations : $\lambda_{SUE} = \lambda_z \left(\frac{c}{c^*} \right)^{\frac{2-3\nu}{3\nu-1}}$ and $\lambda_{SE} = \lambda_z \left(\frac{c}{c^*} \right)^{\frac{3-3\nu}{3\nu-1}}$.

4 Experiment validation using Newtonian fluid

Scaling for DI water in the inertial regime¹⁰ is shown in Fig. S4 where the neck radius R is non-dimensionalized as $R_1^* = R/(\text{Oh}D_o)$ and time as $t_1^* = t\sigma/(\eta\text{Oh}D_o)$ leading to $R_1^* \propto t_1^{0.48}$ which is in good agreement with $R_1^* \propto t_1^{0.50}$.

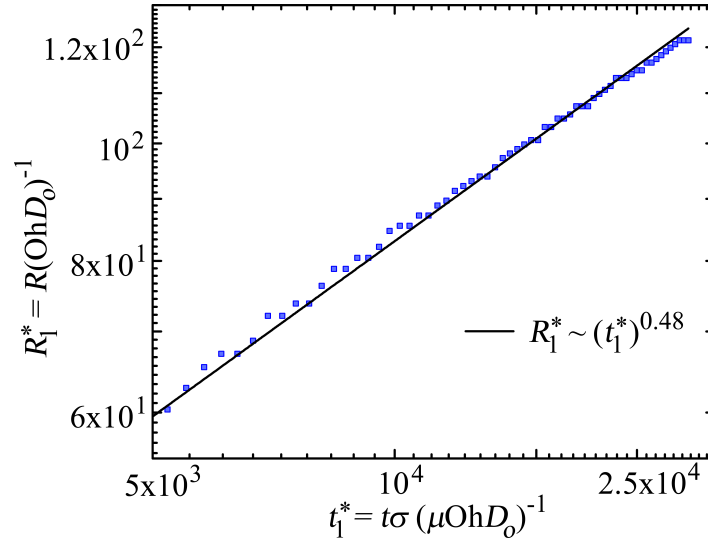


Fig. S4 Scaling of neck radius for DI water in the inertial regime.

5 Theoretical model

To analyse the coalescence phenomenon in polymeric fluids, we appeal to the linear Phan-Thien-Tanner (PTT) model for viscoelastic rheology. The governing equation of linear PTT model is represented in Eq (2) along with the constitutive equations to obtain the relation between stress and rate of deformation given in Eq (3), Eq(4) and momentum equation in radial direction in Eq (5).

$$\lambda \nabla \cdot \boldsymbol{\tau} + \boldsymbol{\tau} \left[1 + \frac{\kappa \lambda}{\eta} \text{Tr}(\boldsymbol{\tau}) \right] = 2\eta \mathbf{D} \quad (2)$$

$$\nabla \tau_{rr} = \frac{\partial \tau_{rr}}{\partial t} + v_r \frac{\partial \tau_{rr}}{\partial r} + v_z \frac{\partial \tau_{rr}}{\partial z} - 2\tau_{rr} \frac{\partial v_r}{\partial r} - 2\tau_{rz} \frac{\partial v_r}{\partial z} \quad (3)$$

$$\nabla \tau_{rz} = \frac{\partial \tau_{rz}}{\partial t} + v_r \frac{\partial \tau_{rz}}{\partial r} + v_z \frac{\partial \tau_{rz}}{\partial z} - \tau_{rr} \frac{\partial v_z}{\partial r} - \tau_{rz} \left(\frac{\partial v_r}{\partial r} + \frac{\partial v_z}{\partial z} \right) - \tau_{zz} \frac{\partial v_r}{\partial z} \quad (4)$$

$$\rho v_r \frac{\partial v_r}{\partial r} = -\frac{\partial p}{\partial r} + \frac{\tau_{rr}}{r} + \frac{\partial \tau_{rr}}{\partial r} + \frac{\partial \tau_{rz}}{\partial z} \quad (5)$$

By assuming flow to be quasi-steady and quasi-radial and the various parameters appearing in the momentum balance, conforming to the linear PTT model, are scaled as $\boldsymbol{\tau} \rightarrow \text{Wi} \bar{\boldsymbol{\tau}}$; $p \rightarrow \text{Wi} \bar{p}$; $R \rightarrow \frac{\bar{R}}{\sqrt{\text{Wi}}}$; $U \rightarrow \sqrt{\text{Wi}} \bar{U}$, where $\boldsymbol{\tau}$ is stress, p is pressure, U is velocity of neck radius and the quantities represented with bars are scaled parameters and Wi is the Weissenberg number. In terms of these scaled parameters, the rr and rz components of the linear PTT model are expressed as:

$$\lambda \text{Wi}^2 \left[\bar{v}_r \frac{\partial \bar{\tau}_{rr}}{\partial \bar{r}} - 2\bar{\tau}_{rr} \frac{\partial \bar{v}_r}{\partial \bar{r}} - 2\bar{\tau}_{rz} \frac{\partial \bar{v}_r}{\partial \bar{z}} \right] + \bar{\tau}_{rr} \text{Wi} \left[1 + \frac{\kappa \lambda \text{Wi}}{\eta} Tr(\bar{\boldsymbol{\tau}}) \right] = 2\eta \text{Wi} \frac{\partial \bar{v}_r}{\partial \bar{r}} \quad (6)$$

$$\lambda \text{Wi}^2 \left[\bar{v}_r \frac{\partial \bar{\tau}_{rz}}{\partial \bar{r}} - \bar{\tau}_{rz} \frac{\partial \bar{v}_r}{\partial \bar{z}} \right] + \bar{\tau}_{rz} \text{Wi} \left[1 + \frac{\kappa \lambda \text{Wi}}{\eta} Tr(\bar{\boldsymbol{\tau}}) \right] = \eta \text{Wi} \frac{\partial \bar{v}_r}{\partial \bar{z}} \quad (7)$$

By making the following approximations: $\lambda \text{Wi}^2 \ll 1$ and $1 + \frac{\kappa \lambda \text{Wi}}{\eta} \bar{\boldsymbol{\tau}} \sim \frac{\kappa \lambda \text{Wi}}{\eta} \bar{\boldsymbol{\tau}}$ (κ is a constant). The stresses are related to velocity gradients as

$$\tau_{rr} \sim \sqrt{\frac{2\eta^2}{\kappa\lambda}} \sqrt{\frac{\partial v_r}{\partial r}} \quad (8)$$

$$\tau_{rz} = \tau_{rr} \frac{\left(\frac{\partial v_r}{\partial z} \right)}{\left(2 \frac{\partial v_r}{\partial r} \right)} \quad (9)$$

Introducing the following scales: $v_r \sim U$, $r \sim R$, $z \sim R$ (R is length scale associated with the neck geometry), Eq (5) effectively reduces to:

$$\rho \frac{U^2}{R} = c_1 \frac{\Delta P}{R} - c_2 \sqrt{\frac{2\eta^2}{\kappa\lambda}} \frac{\sqrt{U}}{R\sqrt{R}} \quad (10)$$

Here, $\Delta P = \sigma \left(\frac{1}{\bar{H}} + \frac{1}{\bar{R}} - \frac{2}{\bar{R}_o} \right)$; $P_1 - P_\infty = \frac{2\sigma}{\bar{R}_o}$, $P_2 - P_\infty = \sigma \left(\frac{1}{\bar{H}} + \frac{1}{\bar{R}} \right)$ (P_1, P_2 being the inside and outside pressures respectively, P_∞ being the atmospheric pressure and σ is the surface tension). Accordingly, (10) gets reduced to:

$$\rho \frac{U^2}{R} = c_1 \frac{\sigma}{HR} - c_2 \sqrt{\frac{2\eta^2}{\kappa\lambda}} \frac{\sqrt{U}}{R\sqrt{R}} \quad (11)$$

Considering the geometric constraint $\frac{H}{R} \approx \frac{R}{2R_o}$ (H is length scale associated with neck geometry and R_o is radius of the drop) as obtained from Fig.4 and introducing the dimensionless parameters $R^* = \frac{R}{\sqrt{v_o \lambda}}$ and $t^* = \frac{t}{\lambda \text{Oh}}$ (where, v_o is the kinematic viscosity, λ is the relaxation time of the solution and $\text{Oh} = \eta / \sqrt{R_o \rho \sigma}$ is the Ohnesorge number), (11) is reduced to:

$$\left(\frac{dR^*}{dt^*} \right)^2 + \frac{A_1}{\sqrt{R^*}} \left(\frac{dR^*}{dt^*} \right)^{\frac{1}{2}} - \frac{A_2}{R^{*2}} = 0 \quad (12)$$

where, $A_1 = \frac{\sqrt{2}}{\sqrt{\kappa}} c_2 \text{Oh}^{\frac{3}{2}}$ and $A_2 = \frac{2\sigma R_o}{\rho v_o^2} c_1 \text{Oh}^2$. (12) is solved using a 4th order Runge-Kutta method. This is suited for non-stiff differential equations of the first order. Since the first order derivative forms a non-linear algebraic equation in itself, it is solved using a numeric solver.

References

- 1 J. Francois, D. Sarazin, T. Schwartz and G. Weill, *Polymer*, 1979, **20**, 969–975.
- 2 V. Tirtaatmadja, G. H. McKinley and J. J. Cooper-White, *Physics of Fluids*, 2006, **18**, 043101.
- 3 I. Lămătic, M. Bercea and S. Morariu, *Revue Roumaine de Chimie*, 2009, **54**, 981–986.
- 4 J. Lee and A. Tripathi, *Analytical Chemistry*, 2005, **77**, 7137–7147.
- 5 O. Arnolds, H. Buggisch, D. Sachsenheimer and N. Willenbacher, *Rheologica Acta*, 2010, **49**, 1207–1217.
- 6 R. B. Bird, R. C. Armstrong and O. Hassager, 1987.
- 7 M. Rubinstein, R. H. Colby *et al.*, *Polymer physics*, Oxford University Press New York, 2003, vol. 23.
- 8 Y. Liu, Y. Jun and V. Steinberg, *Journal of Rheology*, 2009, **53**, 1069–1085.
- 9 F. Del Giudice, G. D’Avino, F. Greco, I. De Santo, P. A. Netti and P. L. Maffettone, *Lab on a Chip*, 2015, **15**, 783–792.
- 10 X. Xia, C. He and P. Zhang, *Proceedings of the National Academy of Sciences*, 2019, **116**, 23467–23472.